This full text paper was peer reviewed at the direction of IEEE Communications Society subject matter experts for publication in the IEEE ICC 2011 proceedings

Optimal Threshold Design for FFR Schemes in Multi-Cell OFDMA Networks*

Zhikun Xu[†‡], Geoffrey Ye Li[‡] and Chenyang Yang[†]

[†]School of Electronics and Information Engineering, Beihang University, Beijing 100191, P. R. China
[‡]School of Electrical and Computer Engineering, Georgia Institute of Technology, Atlanta, GA 30332, USA
Email: xuzhikun@ee.buaa.edu.cn, liye@ece.gatech.edu and cyyang@buaa.edu.cn

***Abstract*—*Fractional frequency reuse* (FFR) is an efficient method to suppress *inter-cell interference* (ICI) in multi-cell OFDMA networks. In this paper, the optimal threshold is designed for FFR schemes to identify cell central and edge users. We first derive throughput of the FFR scheme considering small-scale fading channels and different scheduling strategies. Then we conclude from the analysis and simulation results that the throughput of *maximum normalized SINR* (MNSINR) scheduling is larger than that of *round robin* scheduling, and the optimal thresholds for both scheduling strategies decrease with the increase of cell user number. Simulation results also show that the performance of FFR scheme with the optimal threshold outperforms that with the conventional predefined threshold.**

I. Introduction

Orthogonal frequency division multiple access (OFDMA) technology has been widely applied in the next generation cellular networks, such as WiMAX and 3GPP LTE [1], [2]. Although there is no intra-cell interference among users due to subcarrier orthogonality, *inter-cell interference* (ICI) still exists in OFDMA networks. Especially, with explosive growth of high-quality wireless services, frequency resources are expected to be fully reused among different cells to improve network throughput, which will cause severe ICI and thus serious performance degradation for cell edge users.

In order to guarantee the performance of cell edge users and meanwhile obtain high spectral efficiency over the entire OFDMA network, serval schemes have been proposed, including power control, *fractional frequency reuse* (FFR), scheduling, and MIMO techniques [3]. Among these techniques, FFR is a simple but effective method to reduce ICI. The basic idea of FFR is to apply a small frequency reuse factor to cell central users who have higher SINRs, and apply a large one to cell edge users who have lower SINRs. Through different reuse-factor deployment for users with different SINRs, FFR can achieve good tradeoff between average throughput of the whole network and the performance of cell edge users [4]. According to different adjusting time scale, FFR schemes can be implemented statically or dynamically. For the static FFR scheme, all parameters are configured in advance and keep constant over certain period of time while for the dynamic FFR scheme, some parameters can be adjusted according to instantaneous channel information and traffic load of the networks [5]. In this paper, we concern about the design of static FFR scheme.

In static FFR schemes, selection of important parameters, such as frequency reuse factors, frequency bands for central and edge users and distance or SINR threshold for user identification, affects the performance significantly. However, due to the complexity of optimizing these parameters, they are usually selected based on experiences [4]–[6]. For example, the distance threshold is determined by the criterion that the ratio of average number of central users to the average number of edge users is equal to the ratio of the corresponding subcarriers [4]. In [7], the distance and SINR thresholds are optimized to maximize the average to variance ratio of SINR. In [8], the optimal frequency reuse factor for cell edge region and distance threshold are optimized jointly. Although the threshold has been optimized in [7] and [8], small scale fading channels and scheduling strategies have not been considered, which may play an important role on the threshold design.

In this paper, we will address optimal threshold design for FFR schemes considering two scheduling strategies, *round robin* (RR) scheduling and the *maximum normalized SINR* (MNSINR) scheduling. Specifically, we describe system model and derive the network throughput in Section II. Then the impact of scheduling strategies and cell user number on the design of the optimal SINR threshold is investigated in Section III. Simulation results are provided in Section IV and the paper is concluded in Section V.

II. System and Throughput

In this section, the network model with FFR schemes is first described, and then the average cell throughput is derived.

A. Cell Network Model and FFR Scheme

Consider the downlink of an OFDMA cellular network with the FFR scheme, as shown in Fig. 1. For analytical convenience, the shape of a cell is modeled as a circle with radius, R. We assume that base stations (BS) with omnidirectional antennas are located in the center of cells and users are independently and uniformly distributed in each cell.

For the FFR scheme, users at the center or on the edge of a cell are identified based on the received long term SINRs when

* The work was supported by the Research Gift from Huawei Technologies Co., Ltd., under Grant No. YBWL2010075.

978-1-61284-233-2/11/$26.00 ©2011 IEEE

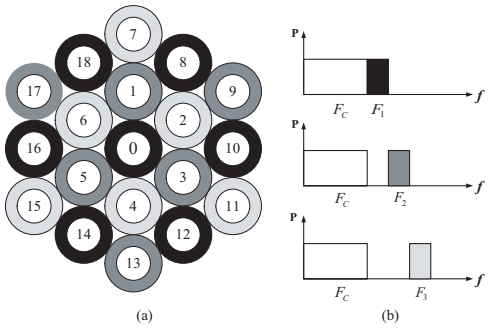

Fig. 1. Network topology and the FFR scheme

the frequency resource is fully reused. A user is regarded as at the center of a cell if its SINR is above a threshold, otherwise, it is regarded as at the edge. Denote $\mathcal{M}_C$ and $\mathcal{M}_E$ to be the index sets of the central users and the edge users, respectively. Then, we have

$$\mathcal{M}_C = \{m:\ \Gamma_m > \Gamma_{th}\} \text{ and } \mathcal{M}_E = \{m:\ \Gamma_m \leq \Gamma_{th}\}, \quad (1)$$

where Γ_m denotes the long term SINR of user m when the frequency resource is fully reused and Γ_{th} represents the SINR threshold. The whole frequency band is divided into two parts for the central and edge users, respectively. The central users are usually with a smaller reuse factor than the edge users. In this paper, we apply reuse factors of one and three for the central and edge users, respectively. As shown in Fig. 1b, $\mathcal{F}_C$ is the band shared among the central users of all the cells and three equal non-overlapped subbands, $\mathcal{F}_1$, $\mathcal{F}_2$ and $\mathcal{F}_3$, are allocated to the edge users of three neighboring cells. Since all cells are similar, we will focus on one cell from now on. The frequency band used by the edge users of concerned cell is denoted as $\mathcal{F}_E$.

B. Channel Model and SINR

In this paper, we assume that all the channels in different links have the same characteristics and consist of large-scale fading part and small-scale fading part. Since long-term SINR threshold is used to distinguish users, the effect of path loss and shadowing fading is combined. In order to simplify the derivation, only path loss is considered in this paper and the derivation taking into account the shadowing is similar. The path loss can be expressed as

$$P_L(d) = \frac{K}{d^\alpha} \quad (2)$$

where d is the distance between the transmitter and the receiver, α is the path loss factor, and K is the pass loss when $d = 1$. Denote $H^j_{m,n}$ to be the frequency response of the small-scale fading channel from BS j to user m on the nth subcarrier, which is subject to complex Gaussian distribution with zero mean and variance σ_h^2.

Then, the SINR of user m on the nth subcarrier can be written as

$$SINR_{m,n} = \frac{P_L(d_{0,m})\|H^0_{m,n}\|^2 P}{N_0\Delta f + I_m}, \quad (3)$$

where $d_{0,m}$ is the distance between user m and BS 0 which is the destination of user m, P denotes the power allocated on each subcarrier, N_0 denotes the power spectral density of noise, Δf is the subcarrier spacing and I_m denotes average power of the interference received by user m, which can be expressed as

$$\begin{aligned} I_m =& \mathbb{E}[\sum_{j\in\mathcal{J}_m} P_L(d_{j,m})\|H^j_{m,n}\|^2 P] \\ =& \sum_{j\in\mathcal{J}_m} P_L(d_{j,m})\sigma_h^2 P. \end{aligned} \quad (4)$$

The value of I_m depends on the position of user m and the interfering cell set $\mathcal{J}_m$.

In order to simplify the analysis, we define long-term SINR of user m as

$$\widetilde{\Gamma}_m \triangleq \mathbb{E}[SINR_{m,n}] = \frac{P_L(d_{0,m})\sigma_h^2 P}{N_0\Delta f + I_m}. \quad (5)$$

Note that $\widetilde{\Gamma}_m$ is different from Γ_m. The former represents the long-term SINR when FFR schemes are used, while the latter is the long-term SINR when the frequency reuse factor is 1. Substituting (5) into (3), we can easily obtain

$$SINR_{m,n} = \widetilde{\Gamma}_m \frac{\|H^0_{m,n}\|^2}{\sigma_h^2} = \widetilde{\Gamma}_m\|\xi_{m,n}\|^2 \quad (6)$$

where $\xi_{m,n}$ is complex Gaussian with zero mean and unit variance.

C. Scheduling Strategies

In this paper, we consider RR and MNSINR scheduling strategies in frequency domain.

The principle of RR scheduling is to select users to access each subcarrier with equal probability. Denote $\widetilde{m}_n$ to be user index which is selected to access the nth subcarrier, then

$$Pr\{\widetilde{m}_n = m\} = \frac{1}{|\mathcal{M}_S|},\ m \in \mathcal{M}_S, n \in \mathcal{F}_S \quad (7)$$

where $\mathcal{M}_S$ can be chosen to be $\mathcal{M}_C$ or $\mathcal{M}_E$ according to the position of user m and $|\mathcal{M}_S|$ is the number of elements in set $\mathcal{M}_S$. Such denotations will be used in the subsequence.

The MNSINR scheduling selects the user with maximum normalized SINR to access each subcarrier, which can be mathematically expressed as

$$\widetilde{m}_n = \arg\max_{m\in\mathcal{M}_S}\{\|\xi_{m,n}\|^2\},\ \ n \in \mathcal{F}_S. \quad (8)$$

The MNSINR scheduling is good approximation of the proportional fair scheduling [6], which not only obtains multiuser diversity to improve the system throughput, but also keeps certain fairness among users.

D. Distribution of Main Random Variables

Before deriving cell throughput, we first clarify distributions of random variables that will be used frequently afterwards. Since users are assumed to be uniformly distributed in a cell, the distance $d_{0,m}$, and the polar angle θ_m are with the

following distributions,

$$f_D(d_{0,m}) = \frac{2d_{0,m}}{R^2 - R_0^2}, \quad R_0 \le d_{0,m} \le R$$
$$f_\Theta(\theta_m) = \frac{1}{2\pi}, \quad 0 \le \theta_m \le 2\pi, \tag{9}$$

where R_0 corresponds to the closest distance that user m can be away from BS 0.

Once $d_{0,m}$ and θ_m are given, the signal power and interference power are known. Therefore, Γ_m is a function of $d_{0,m}$ and θ_m. Based on the analysis in [9], we know Γ_m varies little with θ_m and can be approximately expressed as a monotonous decreasing function of $d_{0,m}$. Assume the SINR threshold in (1), Γ_{th}, corresponds to the distance threshold R_{th}, the probability that user m lies in the central or edge region can be calculated as follows.

$$P_C = Pr\{\Gamma_m > \Gamma_{th}\} = Pr\{R_0 \le d_{J_0,m} < R_{th}\}$$
$$= \int_{R_0}^{R_{th}} f_D(x)\,dx = \frac{R_{th}^2 - R_0^2}{R^2 - R_0^2}, \tag{10}$$

and

$$P_E = Pr\{\Gamma_m \le \Gamma_{th}\} = 1 - P_C = \frac{R^2 - R_{th}^2}{R^2 - R_0^2}. \tag{11}$$

We can further obtain the distribution of user number in cell central and edge regions as follows

$$Pr\{|\mathcal{M}_C| = k\} = \binom{M}{k} P_C^k P_E^{M-k} \tag{12}$$

and

$$Pr\{|\mathcal{M}_E| = k\} = \binom{M}{k} P_E^k P_C^{M-k}, \tag{13}$$

where M is the total user number and $\binom{M}{k}$ denotes combination operation.

Since $\xi_{m,n}$ is subject to Gaussian distribution with zero mean and unit variance, the cumulative distribution function of $\|\xi_{m,n}\|^2$ is

$$F(\gamma) = 1 - \exp(-\gamma).$$

When the RR scheduling is used, the distribution of the small scale fading gain on the nth subcarrier, $\|\xi_{\widetilde{m}_n,n}\|^2$, is

$$F_S^{RR}(\gamma) = \sum_{k \in \mathcal{M}_S} Pr\{\widetilde{m}_n = k\} F(\gamma) = 1 - \exp(-\gamma). \tag{14}$$

When the MNSINR scheduling is used, the distribution of $\|\xi_{\widetilde{m}_n,n}\|^2$ can be expressed as

$$F_S^{MR}(\gamma) = F^{|\mathcal{M}_S|}(\gamma) = [1 - \exp(-\gamma)]^{|\mathcal{M}_S|}. \tag{15}$$

E. Theoretical Throughput Calculation

In this subsection, the cell throughput is calculated based on the assumption that the ICI is with complex Gaussian distribution. Although such assumption may be invalid in reality, the Gaussian interference is the worst case and the calculated throughput under this assumption can be regarded as the lower bound of the cell throughput [10].

If ICI is Gaussian, according to the Shannon's formula, the instantaneous throughput in cell central region can be expressed as

$$C_C = \Delta f \sum_{n \in \mathcal{F}_C} \log_2(1 + SINR_{\tilde{m}_n,n}). \tag{16}$$

Then, the average throughput in cell central region can be expressed as

$$\overline{C}_C = \mathbb{E}[\Delta f \sum_{n \in \mathcal{F}_C} \log_2(1 + SINR_{\tilde{m}_n,n})] \tag{17}$$
$$= \Delta f \sum_{k=1}^{M} Pr\{|\mathcal{M}_C| = k\} \mathbb{E}_{\mathbf{V}_C}[\sum_{n \in \mathcal{F}_C} \log_2(1 + \widetilde{\Gamma}_{\tilde{m}_n} \|\xi_{\tilde{m}_n,n}\|^2)]$$

where $\mathbf{V}_C$ represents the set of all random variables in the expression of instantaneous throughput.

It is necessary to clarify the random variables in $\mathbf{V}_C$. From the description in the subsection D of previous section, we know that $\widetilde{\Gamma}_{\widetilde{m}_n}$ is a function of the random variable $d_{0,\widetilde{m}_n}$. Therefore, the set $\mathbf{V}_C$ includes $\{d_{0,\widetilde{m}_n}\}_{n \in \mathcal{F}_C}$ and $\{\|\xi_{\widetilde{m}_n,n}\|^2\}_{n \in \mathcal{F}_C}$. It is readily to prove that random variables, $\{d_{0,\widetilde{m}_n}\}_{n \in \mathcal{F}_C}$ and $\{\|\xi_{\widetilde{m}_n,n}\|^2\}_{n \in \mathcal{F}_C}$, are independent of the indexes of user and subcarrier.

Therefore, we can further simplify (17) as

$$\overline{C}_C = \Delta f |\mathcal{F}_C| \sum_{k=1}^{M} Pr\{|\mathcal{M}_C| = k\} \mathbb{E}_{\mathbf{V}_C}[\log_2(1 + \widetilde{\Gamma}_C \|\xi_C\|^2)], \tag{18}$$

where $\widetilde{\Gamma}_C$ and $\|\xi_C\|^2$ have the same distributions as $\{\widetilde{\Gamma}_{m,n}\}_{n \in \mathcal{F}_C}$ and $\{\|\xi_{\tilde{m}_n,n}\|^2\}_{n \in \mathcal{F}_C}$, respectively. Similarly, the average throughput in the cell edge region can be expressed as

$$\overline{C}_E = \Delta f |\mathcal{F}_E| \sum_{k=1}^{M} Pr\{|\mathcal{M}_E| = k\} \mathbb{E}_{\mathbf{V}_E}[\log_2(1 + \widetilde{\Gamma}_E \|\xi_E\|^2)]. \tag{19}$$

Consequently, the average cell throughput is

$$\overline{C} = \overline{C}_C + \overline{C}_E \tag{20}$$
$$= \Delta f |\mathcal{F}_C| \sum_{k=1}^{M} Pr\{|\mathcal{M}_C| = k\} \mathbb{E}_{\mathbf{V}_C}[\log_2(1 + \widetilde{\Gamma}_C \|\xi_C\|^2)]$$
$$+ \Delta f |\mathcal{F}_E| \sum_{k=1}^{M} Pr\{|\mathcal{M}_E| = k\} \mathbb{E}_{\mathbf{V}_E}[\log_2(1 + \widetilde{\Gamma}_E \|\xi_E\|^2)].$$

III. Throughput Analysis and Threshold Optimization

In this section, we will analyze the impact of different scheduling strategies and cell user number on cell throughput and optimal threshold.

When the RR scheduling is used, we know that $\mathbb{E}_{\mathbf{V}_S}\{\log_2(1 + \widetilde{\Gamma}_S \|\xi_S\|^2)\}$ in (20) is independent of $|\mathcal{M}_S|$ based on the distribution of $\|\xi_{\widetilde{m}_n,n}\|^2$ in (14). Then the average throughput with RR scheduling can be expressed as

$$\overline{C}_R = \Delta f |\mathcal{F}_C| (1 - P_E^M) \mathbb{E}_{\mathbf{V}_C}[\log_2(1 + \widetilde{\Gamma}_C \|\xi_C\|^2)] \tag{21}$$
$$+ \Delta f |\mathcal{F}_E| (1 - P_C^M) \mathbb{E}_{\mathbf{V}_E}[\log_2(1 + \widetilde{\Gamma}_E \|\xi_E\|^2)].$$

It is easy to derive that

$$\mathbb{E}_{\mathbf{V}_C}[\log_2(1+\widetilde{\Gamma}_C\|\xi_C\|^2)] = \frac{1}{\ln 2}\frac{\int_{R_0}^{R_{th}} I_1(\frac{1}{\widetilde{\Gamma}_C(x)})\frac{2x}{\widetilde{\Gamma}_C(x)}dx}{(R_{th}^2-R_0^2)} \tag{22}$$

and

$$\mathbb{E}_{\mathbf{V}_E}[\log_2(1+\widetilde{\Gamma}_E\|\xi_E\|^2)] = \frac{1}{\ln 2}\frac{\int_{R_{th}}^{R} I_1(\frac{1}{\widetilde{\Gamma}_E(x)})\frac{2x}{\widetilde{\Gamma}_E(x)}dx}{(R^2-R_{th}^2)} \tag{23}$$

where $I_1(\mu)$ is defined as $I_1(\mu)=\int_0^{+\infty}\ln(1+t)e^{-\mu t}dt$ and (14) is used for derivation. Note that we rewrite $\widetilde{\Gamma}_S$ as $\widetilde{\Gamma}_S(x)$ to emphasize that $\widetilde{\Gamma}_S$ is the function of the distance, x. After substituting (22) and (23) into (21), the accurate throughput of the RR scheduler is expressed as a function of the threshold R_{th}.

When the MNSINR scheduler is used, the accurate throughput cannot be easily derived because the value of expression $\mathbb{E}_{\mathbf{V}_S}[\log_2(1+\widetilde{\Gamma}_S\|\xi_S\|^2)]$ in (20) depends on $|\mathcal{M}_S|$. Therefore, we use the upper bound as an approximation to gain some insights.

From Jensen's inequality, we can obtain that

$$\mathbb{E}_{\mathbf{V}_S}[\log_2(1+\widetilde{\Gamma}_S\|\xi_S\|^2)] \le \mathbb{E}_{\widetilde{\Gamma}_S}\{\log_2(1+\widetilde{\Gamma}_S\mathbb{E}_{\|\xi_S\|^2}[\|\xi_S\|^2])\}.$$

Since $\widetilde{\Gamma}_S$ is usually very large in FFR schemes, we can further simplify the expression as follows

$$\begin{aligned}&\mathbb{E}_{\mathbf{V}_S}[\log_2(1+\widetilde{\Gamma}_S\|\xi_S\|^2)] \le \mathbb{E}_{\widetilde{\Gamma}_S}\{\log_2(\widetilde{\Gamma}_S\mathbb{E}_{\|\xi_S\|^2}[\|\xi_S\|^2])\}\\ &= \mathbb{E}_{\widetilde{\Gamma}_S}[\log_2\widetilde{\Gamma}_S] + \log_2(\mathbb{E}_{\|\xi_S\|^2}[\|\xi_S\|^2]).\end{aligned} \tag{24}$$

Substituting (24) into (20), we can obtain equation (25) at the top of next page, where $\mathbb{E}_{\|\xi_S\|^2}[\|\xi_S\|^2] = \sum_{k=1}^{|\mathcal{M}_S|}\frac{1}{k}$ and $\mathbb{E}_{\widetilde{\Gamma}_C}[\log_2(\widetilde{\Gamma}_C)] = \frac{\int_{R_0}^{R_{th}} 2x\log_2\widetilde{\Gamma}_C(x)dx}{R_{th}^2-R_0^2}$ and $\mathbb{E}_{\widetilde{\Gamma}_E}[\log_2(\widetilde{\Gamma}_E)] = \frac{\int_{R_{th}}^{R} 2x\log_2\widetilde{\Gamma}_E(x)dx}{R^2-R_{th}^2}$. When expressions $(10)-(13)$ are substituted into the right side of (25), the upper bound can be expressed as a function of R_{th}. We use it as the approximate throughput of the MNSINR scheduling, which will be proved a good approximation from the following simulation results.

Comparing (21) with (25), we can find that the throughput of MNSINR scheduling is larger than that of RR scheduling and both of them increase with the user number M. Due to the complexity of throughput expressions, the impact of user number on the threshold, R_{th}, cannot be observed directly. We have proved that the optimal threshold decreases with the increase of M. Due to the space limitation, we cannot provide the detailed proof here. However, from the simulation results, the same conclusion can also be obtained.

IV. NUMERICAL AND SIMULATION RESULTS

In this section, we will provide numerical and simulation results for FFR schemes with different scheduling strategies and different user numbers. In our simulation, we consider 19 cells that have the same size and deployment. The threshold in all figures refers to R_{th} in previous discussion and main parameters are listed in Table I.

TABLE I
SIMULATION SETUP

Cell Parameters	
Number of Cells	19
Cell Radius	500m
Antennas	SISO
Antenna Gain at BS	14dB
Minimum Distance from UE to BS (R_0)	25m
OFDM Parameters	
Total Bandwidth	20MHz
Number of Subcarriers	512
Number of Central Subcarriers N_C	257
Number of Edge Subcarriers N_E	85
Channel Model	
Path Loss	35+38log$d$
Multi-path Model	Rayleigh fading with $\sigma_h^2=1$
Power Parameters	
Transmit Power of BS	49dBm
Thermal Noise Power Spectral Density	-174dBm/Hz
Noise Amplification Coefficient of UE	7dBi

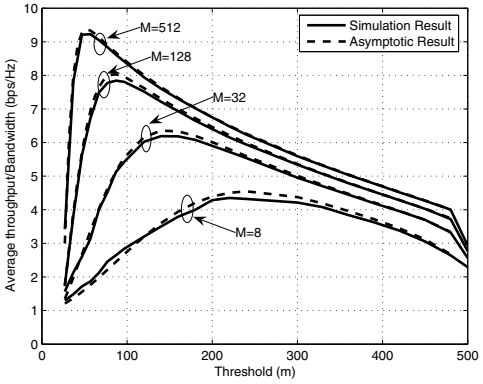

Fig. 2. Comparison between numerical results and simulation results when the MNSINR scheduling is used

We first compare simulation results with numerical results to demonstrate that the approximation in (25) is reasonable. From Figure 2, we can see the gap between these two results is very small, which validates that the approximation is very accurate for the MNSINR scheduling.

Figure 3 illustrates the performance of the RR and MNSINR scheduling strategies. It can be observed that the throughput of both strategies increases with user number M and the throughput of the MNSINR scheduling is larger than that of the RR scheduling. The reason is that the MNSINR scheduling can obtain the diversity gain from the selection of the small scale fading channel gains but the RR scheduling cannot. We can also see that the optimal threshold becomes smaller with increase of M and it goes towards R_0 when $M\to\infty$.

In order to highlight the importance of threshold design considering small-scale fading channels and scheduling strategies,

$$\begin{aligned}\overline{C}_M \simeq & \Delta f\{|\mathcal{F}_C|\sum_{k=1}^{M} Pr\{|\mathcal{M}_C|=k\}\{\mathbb{E}_{\widetilde{\Gamma}_C}[\log_2\widetilde{\Gamma}_C]+\log_2(\mathbb{E}_{\|\xi_C\|^2}[\|\xi_C\|^2])\} \\ & + \Delta f|\mathcal{F}_E|\sum_{k=1}^{M} Pr\{|\mathcal{M}_E|=k\}\{\mathbb{E}_{\widetilde{\Gamma}_E}[\log_2\widetilde{\Gamma}_E]+\log_2(\mathbb{E}_{\|\xi_E\|^2}[\|\xi_E\|^2])\}\} \\ = & \Delta f|\mathcal{F}_C|(1-P_E^M)\mathbb{E}_{\widetilde{\Gamma}_C}\{\log_2\widetilde{\Gamma}_C\}+\Delta f|\mathcal{F}_E|(1-P_C^M)\mathbb{E}_{\widetilde{\Gamma}_E}\{\log_2\widetilde{\Gamma}_E\} \\ & + \Delta f|\mathcal{F}_C|\sum_{k=1}^{M} Pr\{|\mathcal{M}_C|=k\}\log_2(\mathbb{E}_{\|\xi_C\|^2}[\|\xi_C\|^2])+\Delta f|\mathcal{F}_E|\sum_{k=1}^{M} Pr\{|\mathcal{M}_E|=k\}\log_2(\mathbb{E}_{\|\xi_E\|^2}[\|\xi_E\|^2])\end{aligned} \tag{25}$$

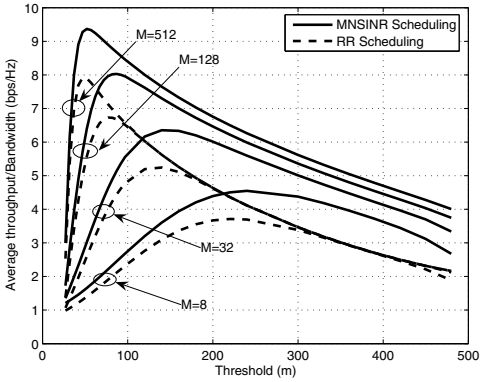

Fig. 3. Comparison between the throughput of RR scheduling and the throughput of MNSINR scheduling

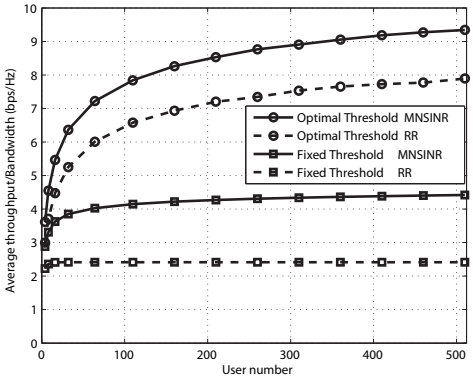

Fig. 4. Comparison between the throughput with the optimal threshold and that with the fixed threshold

we compare the performance of FFR scheme using the optimal threshold with that using a fixed threshold. The fixed threshold is based on the principle that the ratio of average number of central users to the average number of edge users is the ratio of the corresponding subcarriers [4], i.e. $\frac{T_f^2-R_0^2}{R^2-T_f^2}=\frac{|\mathcal{F}_C|}{|\mathcal{F}_E|}$, where T_f is the fixed threshold. The throughput versus user number is shown in Figure 4. As we expect, the performance of the optimal threshold outperforms that of the fixed threshold, which means FFR schemes with the optimal threshold can obtain more diversity gains than that with the fixed threshold.

V. Conclusion

In this paper, we have designed the optimal threshold that is used to identify the cell central and edge users for FFR schemes in mutli-cell OFDMA-based networks. First, the average throughput of FFR scheme with the RR or MNSINR scheduling has been derived. From analysis and simulation results, we have found that both the throughput of the RR scheduling and the throughput of the MNSINR scheduling increase with the user number while the optimal threshold decreases with the increase of the user number. It can be observed that the cell throughput with the optimal threshold considering small-scale fading channels and scheduling strategies outperforms that with a fixed threshold.

References

[1] F. Wang, A. Ghosh, C. Sankaran, Fleming, F. Hsieh, and S. J. Benes, "Mobile WiMAX systems: performance and evolution," *IEEE Commun. Mag.*, vol. 46, no. 10, pp. 41–49, Oct. 2008.

[2] D. Astely, E. Dahlman, A. Furuskar, Y. Jading, M. Lindstrom, and S. Parkvall, "LTE: the evolution of mobile broadband," *IEEE Commun. Mag.*, vol. 47, no. 4, pp. 44–51, Apr. 2009.

[3] G. Boudreau, J. Panicker, N. Guo, R. Chang, N. Wang, and S. Vrzic, "Interference coordination and cancellation for 4G networks," *IEEE Commun. Mag.*, vol. 47, no. 4, pp. 74–81, Apr. 2009.

[4] H. Lei, L. Zhang, and D. Yang, "A novel multi-cell OFDMA system structure using fractional frequency reuse," in *IEEE Int. Symp. Personal, Indoor Mobile Radio Commun.*, Sept. 2007, pp. 1–5.

[5] R. Y. Chang, Z. Tao, J. Zhang, and C.-C. J. Kuo, "A graph approach to dynamic fractional frequency reuse (FFR) in multi-cell OFDMA networks," in *Proc. IEEE Int. Conf. Commun.*, May 2009, pp. 1–6.

[6] H. Fujii and H. Yoshino, "Theoretical capacity and outage rate of OFDMA cellular system with fractional frequency reuse," in *Proc. IEEE Veh. Technol. Conf.*, 2008, pp. 1676–1680.

[7] A. Najjar, N. Hamdi, and A. Bouallegue, "Efficient frequency reuse scheme for multi-cell OFDMA systems," in *IEEE Symp. Comput. Commun.*, Jul. 2009, pp. 261–265.

[8] M. Assaad, "Optimal fractional frequency reuse (FFR) in multicellular OFDMA system," in *Proc. IEEE Veh. Technol. Conf.*, 2008, pp. 1–5.

[9] M. Maqbool, P. Godlewski, M. Coupechoux, and J.-M. Kelif, "Analytical performance evaluation of various frequency reuse and scheduling schemes in cellular OFDMA networks," *Performance Evaluation*, vol. 67, no. 4, pp. 318–337, Apr. 2010.

[10] M.-S. Alouini and A. J. Goldsmith, "Capacity of rayleigh fading channels under different adaptive transmission and diversity-combining techniques," *IEEE Trans. Veh. Technol.*, vol. 48, no. 4, pp. 1165–1180, Jul. 1999.